CHEMISTRY OF MATERIALS
Cite This: Chem. Mater. 2018, 30, 2544−2549
Article
pubs.acs.org/cm

Modulation of Carrier Type in Nanocrystal-in-Matrix Composites by Interfacial Doping

Richa Sharma,[†,⊥] April M. Sawvel,[†] Bastian Barton,[†] Angang Dong,[†] Raffaella Buonsanti,[†] Anna Llordes,[†] Eric Schaible,[‡] Stephanus Axnanda,[‡] Zhi Liu,[‡] Jeffrey J. Urban,[†] Dennis Nordlund,[§] Christian Kisielowski,[†] and Delia J. Milliron*[,†,∥]

[†]The Molecular Foundry, Lawrence Berkeley National Laboratory, Berkeley, California 94720, United States
[‡]Advanced Light Source, Lawrence Berkeley National Laboratory, Berkeley, California 94720, United States
[§]Stanford Synchrotron Radiation Laboratory, P.O. Box 20450, Stanford, California 94309, United States
[∥]McKetta Department of Chemical Engineering, The University of Texas at Austin, Austin, Texas 78712, United States

Supporting Information

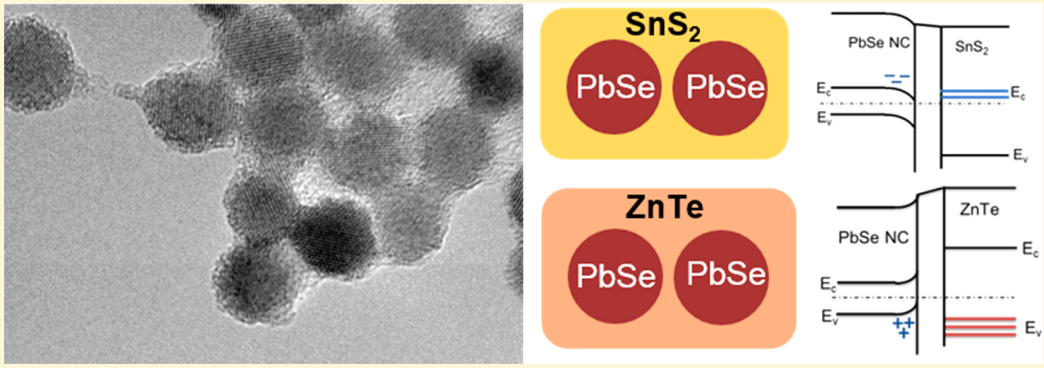

ABSTRACT: Inorganic nanocomposites synthesized by combination of colloidal nanocrystals (NCs) and inorganic clusters have recently emerged as new materials with novel and unique functionalities. Much of the demonstrated promise of nanocomposites derives from the unique interactions between NC and matrix components—this generates new material properties, which direct unique transport behavior in the overall solid or nanocomposite—be it mass, charge, or heat. While measured empirically, it has remained largely impossible to take an a priori look at material properties and use those as a guideline to design desired transport behavior. Fundamentally, this is because the structural and electronic changes manifest at those interfaces have remained hidden from examination. Here, we provide experimental evidence that transport behavior in nanocrystal-in-matrix (NIM) composites is dictated primarily by interfacial charge transfer associated with electronic and structural reconstructions as the composite forms. Our approach building continuous composite superlattices serves as a starting point for systematic probing of the nanointerface of NIM composites via ultrathin films. A combination of field effect transistor device characterization and photoemission spectroscopy reveals the systematic dependence of the polarity of charge transfer on the selection of matrix materials in NIM composites. We use this insight to combine, by design, different components to tune the carrier type in NIM composites.

Inorganic nanocomposites have recently emerged as exciting new materials because of their compositionally tunable electronic and optical properties. Several innovative surface chemistries have been developed for nanocrystal-in-matrix (NIM) nanocomposite synthesis to passivate the electronic trap states that are associated with the nanocrystal (NC) surface. Furthermore, the combination of intrinsic properties of the constituent materials and emergent properties of their interface provides novel and useful functionalities to the synthesized nanocomposite. Although several recent papers[1−8] have focused on the idea of surface doping in NC films, a complete understanding of how charge transport at the embedded interfaces can dominate behavior is needed to advance this idea into practical applications. In this paper, we report progress in this direction. Specifically, our main contribution is to demonstrate how the selection of a matrix in a dense NIM composite can be used to tune the carrier type by varying the nature of the electronic interaction at the interfaces. We use the field effect transistor and photoemission spectroscopy (PES) with low excitation energy (i.e., ultraviolet PES or UPS) measurements to show that the NIM composition can control the electronic level alignments at the

Received: November 7, 2017
Revised: March 22, 2018
Published: April 2, 2018

DOI: 10.1021/acs.chemmater.7b04689
Chem. Mater. 2018, 30, 2544−2549

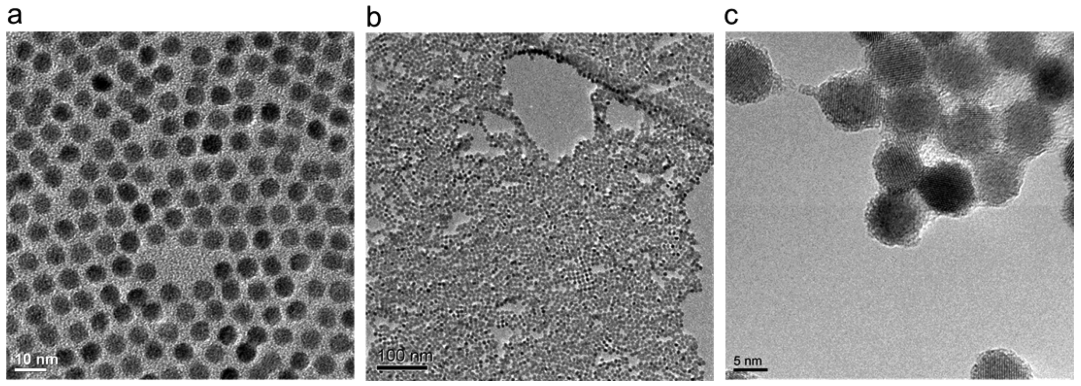

Figure 1. TEM characterization of nanocomposites. a, PbSe with organic ligands; b, PbSe-in-$(N_2H_5)_4Sn_2S_6$; c, PbSe-in-$(N_2H_5)_4Ge_2S_6$.

interface, thus enabling effective tailoring of charge carrier polarity. Thus, the resulting interface doping is enabled by the electronic reconstruction at the continuous nanocrystal-matrix interface, and the high density of that interface dominates the macroscopic observables, namely, charge carrier type and concentration.

We control the carrier type in PbSe NC-in-matrix thin film transistors (TFTs) from n-type and p-type to bipolar by varying the matrix between SnS_2, ZnTe, and $(N_2H_5)_4Ge_2S_6$, respectively. This sweeping tunability provides insights to guide the design and component selection in inorganic nanocomposites. Each of the three matrix materials was chemically prepared from chalcogenidometallates (ChaM) precursors, which have been shown to yield electronic quality inorganic semiconductors upon thermal annealing.[9−11] Note that, in contrast to the SnS_2 and ZnTe matrices, we did not anneal the ChaMs in the case of $(N_2H_5)_4Ge_2S_6$. The compound $(N_2H_5)_4Ge_2S_6$ is itself a molecular species with a large band gap and a minimum thermal treatment allows us to retain its electronic properties as such. In this way, we minimize the perturbation to the electronic properties of the NCs, effectively decoupling the NC electronic structure and properties from the $(N_2H_5)_4Ge_2S_6$ matrix. Nonetheless, for the sake of completeness, we have included the electronic properties of an annealed device based on this ChaM (with the matrix effectively converted to GeS_2), as shown in Figure S5.

In previous studies, surface charge transfer doping[12] has been shown to be a powerful mechanism to tune the electronic properties of NCs.[1−3,5−8,13,14] In this work, we focus on applying this concept to understand and control the electronic reconstruction at the NC−matrix interface that leads to the modulation of charge carrier type in PbSe NCs embedded in SnS_2, $(N_2H_5)_4Ge_2S_6$, and ZnTe inorganic matrices. We use UPS to measure the energy level alignment between the NCs and the matrix that is responsible for charge transfer doping, which provides a solid foundation for component selection in tuning the NIM interface. Charge transfer between the matrix materials and the NCs leads to electronic doping and, because of the dense, regular arrangement of the NCs, the macroscopic electronic behavior of the composite reflects these local changes in charge states. We are therefore able to apply this interfacial doping concept to modulate the carrier type in PbSe NIM thin film devices by varying the selection of matrix material.

In our previous work, we fabricated continuous, ultrathin films of NIM composites by carrying out ligand exchange on NC assemblies floating at a liquid surface.[15] To best demonstrate the interplay between interface effects and manifest electronic behavior, we chose PbSe NCs, which are known to exhibit ambipolar transport under some conditions and which have well-studied surface chemistry.[16−21] In this approach, the organic ligands native to the NCs are replaced with inorganic ChaMs of composition $(N_2H_5)_4Sn_2S_6$ or $(N_2H_5)_4Ge_2S_6$, or extended inorganic chains of $(N_2H_4)_2ZnTe$.[9] The free-floating films allow local reorganization of NCs during the ligand exchange process. This limits the formation of cracks and defects and enables the growth of membranes with regularly ordered structure as confirmed by SEM, TEM, and GISAXS measurements, as demonstrated in our previous work.[15] To illustrate the structure of the thin film nanocomposites, TEM and SEM images are shown in Figure 1 and Figure S2.

Inspired by literature reports of surface charge transfer doping, we sought to manipulate the electronic properties in these ultrathin composites by selecting component materials for their range of anticipated energy level alignment. PbSe NC assemblies with organic ligands have been reported to show ambipolar charge transport,[22,23] making these an excellent choice for our investigation. In our work, we selected quantum confined 7 nm PbSe NCs, which exhibit a substantial surface area that we could leverage to tune the macroscopic electronic properties based on interfacial interactions. The three ChaMs, $(N_2H_5)_4Sn_2S_6$, $(N_2H_5)_4Ge_2S_6$, and $(N_2H_4)_2ZnTe$, were selected to vary the interaction with the PbSe nanocrystals. These ChaMs can be thermally decomposed to the corresponding inorganic matrix (SnS_2, GeS_2, and ZnTe) upon annealing following ligand exchange. The synthetic methods are fully described in our previous work[15] and Supporting Information.[9−11,24]

We emphasize that the nanocomposite films fabricated in this work are monolayers of NCs with no excessive ChaMs or inorganic matrix. The ChaM-derived matrix material is primarily present at the interface and NC surface, as evident from the less than 1 nm distance between neighboring NCs in TEM images and also the AFM characterization of NIM films showing ca. 8 nm height.[15] This morphology is consistent with our main objective of fabricating nanocomposites with a high density of NIM nanointerfaces, both to facilitated strong tuning of properties and to make the interfaces accessible for probing electronic reconstruction. Specifically, in this work, we use UPS to probe the outermost valence bands of the NCs and inorganic matrix and the band alignment at their interface.

We hypothesized that the different matrix materials would interact electronically with the PbSe NCs to modify the electronic levels relevant to conduction of electrons and holes.

DOI: 10.1021/acs.chemmater.7b04689
Chem. Mater. 2018, 30, 2544−2549

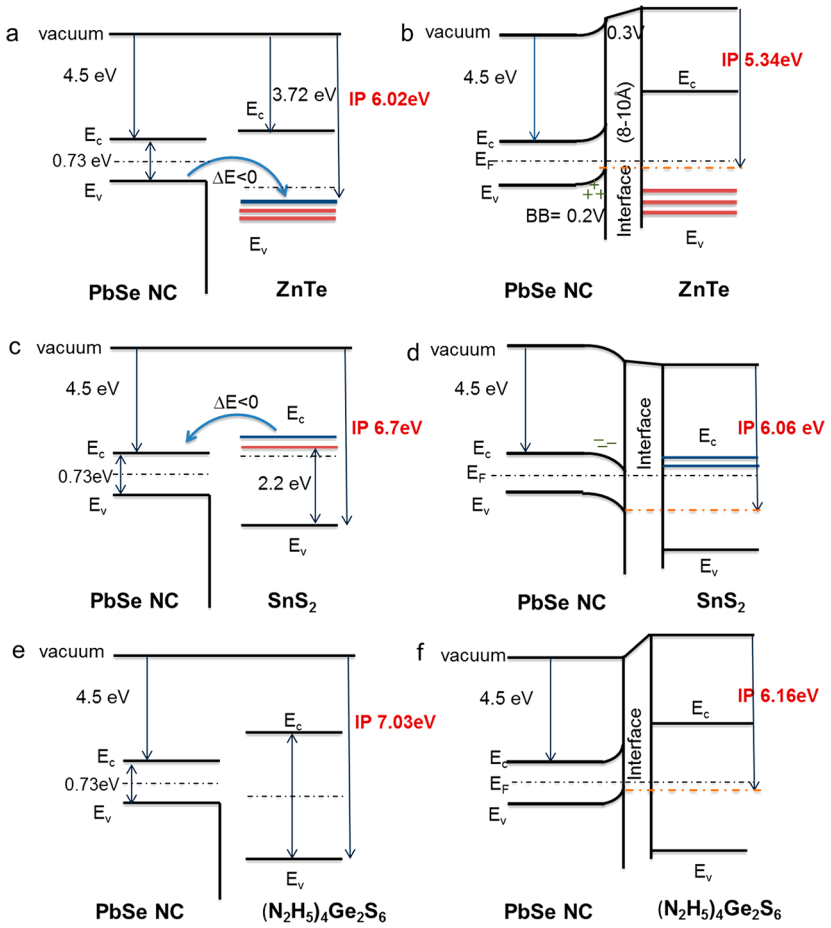

Figure 2. Schematic energy level diagrams at the interface for PbSe-in-ZnTe, PbSe-in-SnS_2, and PbSe-in-$(N_2H_5)_4Ge_2S_6$. a, c, e, Before surface transfer doping of PbSe nanocrystals. b, d, f, After surface transfer doping. E_c and E_v are the conduction and valence band edges, respectively.

To probe the electronic structure of the NC−matrix interface we used UPS. The ultrathin, highly uniform films accessible by our unique fabrication strategy are ideal for quantitative UPS analysis. UPS allows us to determine the interfacial electronic energy-level alignment and predict how surface charge reorganization could give rise to electronic doping. To accomplish these objectives, we use UPS to determine work functions and valence band maxima (VBM) of the matrix materials alone and with embedded NCs. In UPS, we measure the kinetic energy (KE) distribution of the photoelectrons that are primarily emitted from the valence bands. Figure S1 shows the UPS spectra of the various matrix materials. The low KE edge is the secondary-electron cutoff (SECO), which allows us to determine the work function, while the high KE data yield the valence band maximum (VBM). In our ultrathin nanocomposite films (here supported on highly doped silicon wafers to avoid charging during UPS analysis), UPS almost exclusively probes the interface of the matrix and PbSe NCs. This is because the mean free path of these low KE photoelectrons is extremely short (~5 Å). The spectra thus remain free from features of the underlying silicon valence band, which could otherwise complicate interpretation. (The VBM of the native SiO_2 appears at higher binding energy and does not interfere with our analysis.) To achieve high surface sensitivity and fine energy resolution, we performed the UPS experiments with synchrotron radiation using an incident photon energy of 80 eV. The near-surface valence electronic energy levels are determined relative to the Fermi level of gold as the reference metal. Thereafter, we determine the ionization energy (IE), which is the energy difference between VBM of a semiconductor material and the vacuum level. We use the IE measurements for the pure matrix materials and the nanocomposites in conjunction with the values of the band gaps available from the literature[25,26] to evaluate the energy band alignment across the interface.

The interfacial band alignment deduced from UPS shows we can systematically tune the energy level shifts at the NC−matrix interface by varying the matrix composition. The data from the component materials allows us to construct hypothetical energy level alignments absent electronic reconstruction, while measurements of the composite films reveal shifts due to interfacial charge transfer. This charge transfer process is illustrated in Figure 2a,b for the PbSe-in-ZnTe nanocomposite. ZnTe is a p-type semiconductor[9] with its Fermi level close to the VBM and some unoccupied states (holes) in the valence band. PbSe NC energy levels are drawn from the literature to complement our measurements of the matrix materials and composites.[27,28] As PbSe NCs and ZnTe are brought in contact, the Fermi energy difference between them will drive electrons from the PbSe NC valence band to the partially filled valence band of the ZnTe. The energy difference between the top of valence bands of ZnTe and PbSe NC is expected to be negative ($\Delta E < 0$) thus making this electron transfer process energetically favorable. This electron transfer at the PbSe NC and ZnTe interface implies p-type doping of PbSe NC. At the interface, a space charge layer is formed due to the charge

DOI: 10.1021/acs.chemmater.7b04689
Chem. Mater. 2018, 30, 2544−2549

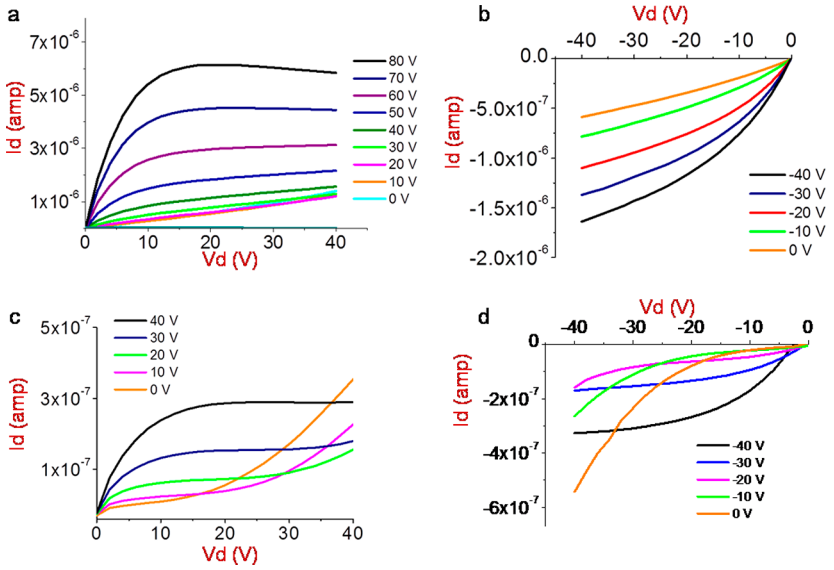

Figure 3. Output characteristics of TFTs with PbSe nanocomposite channel layers. a, PbSe-in-SnS_2, b, PbSe-in-ZnTe, and c, d, PbSe-in-$(N_2H_5)_4Ge_2S_6$. The legend indicates the gate voltage applied. Analysis of these data indicate the electron mobility in PbSe-in-SnS_2 nanocomposite is 0.73 $cm^2\ V^{-1}\ s^{-1}$ (μ_{lin}), hole mobility in PbSe-in-ZnTe is 0.027 $cm^2\ V^{-1}\ s^{-1}$ (μ_{lin}), and electron and hole mobilities in PbSe-in-$(N_2H_5)_4Ge_2S_6$ are 0.007 $cm^2\ V^{-1}\ s^{-1}$ (μ_{lin}) and 0.002 $cm^2\ V^{-1}\ s^{-1}$ (μ_{lin}), respectively.

transfer, which results in energy band bending at the surface of PbSe NCs at electrochemical equilibrium. We therefore propose that the IE measured for the PbSe-in-ZnTe composites (5.3 eV) is the energy difference at equilibrium between the vacuum level and the bent valence band at the surface of the PbSe NCs. Charge transfer and mutual electronic polarization of the two materials effectively shifts the vacuum level at their interface. We can rationalize the measured 5.3 eV IE as arising from 0.2 eV band bending and 0.3 eV shift in vacuum level at equilibrium, both arising from interfacial charge transfer.

Note that this description of the interfacial electronic reorganization does not rely on a specific mechanistic model; however, it is consistent with the induced density of interface states (IDIS) model, in which resonant interactions at the interface facilitate the charge transfer process driven, as in our description, by an offset in Fermi levels between the two materials when isolated from each other.[12,29] On the other hand, the integer charge transfer (ICT) model, invoked in some cases for weak electronic coupling at the interface, is not likely applicable as it involves the formation of discrete localized charged states in one (or both) materials.[30] Typically, organic molecular materials with strong electron−phonon coupling can form polaronic states in their band gap that could be implicated in the ICT model, while our inorganic composites suggest no such likely candidates for localized states.

Following the interpretation approach used to analyze our results for the PbSe-in-ZnTe nanocomposite, Figure 2c−f illustrates the charge transfer reconstruction for PbSe-in-SnS_2 and PbSe-in-$(N_2H_5)_4Ge_2S_6$ nanocomposites. SnS_2 is an n-type semiconductor with its Fermi level close the bottom of its conduction band and some occupied states (electrons) in these bands. Before charge transfer, the Fermi level of PbSe NCs is at a lower energy than the Fermi level of SnS_2 and the energy difference between the bottom of their conduction bands is negative ($\Delta E < 0$) as shown in Figure 2c. Thus, the transfer of electrons from the partially occupied conduction band of SnS_2 to the unoccupied conduction band of PbSe NC is energetically favored. This electron transfer at the PbSe NC and SnS_2 interface suggests n-type doping of the PbSe NC. At equilibrium, the band edges at the PbSe surface bend downward. Here, we propose that the measured IE of the nanocomposite is the energy difference between the bent PbSe valence band and the SnS_2 vacuum level (Figure 2d). We measure a lower value of IE for the nanocomposite than for pristine SnS_2, which supports our hypothesis of surface charge transfer. For our third nanocomposite of PbSe-in-$(N_2H_5)_4Ge_2S_6$, the band alignment is illustrated in Figure 2e,f. $(N_2H_5)_4Ge_2S_6$ is a wide bandgap molecular solid ($\Delta E_g > 3$ eV). We hypothesize there should be negligible charge transfer reconstruction at the interface of PbSe and $(N_2H_5)_4Ge_2S_6$ due to the large energy difference between their respective energy band edges. A very small number of electrons transferred from PbSe NCs to $(N_2H_5)_4Ge_2S_6$ will align their Fermi levels at equilibrium. Using UPS, we measure 7 eV IE for $(N_2H_5)_4Ge_2S_6$ films and 6.1 eV IE for the associated nanocomposite. We propose the measured IE for the nanocomposite reflects the energy difference at equilibrium between the vacuum level of $(N_2H_5)_4Ge_2S_6$ matrix and the bent valence band at the surface of the PbSe NCs. These measurements suggest PbSe NCs in this nanocomposite will retain their ambipolar characteristics due to negligible charge transfer at their interface.

The high density of continuous interface in our nanocomposites means the interface region can dominate macroscopic observables such as charge transport.[31] Thus, we characterize the functional impact of surface charge transfer doping by assessing the electronic properties of the three inorganic nanocomposites. To evaluate the electronic properties we fabricate TFTs. The nanocomposite thin films that were prepared by the free-floating ligand exchange method were transferred on to highly doped silicon wafers with 200 nm SiO_2 thermal gate oxide followed by source and drain electrode patterning. Both source and drain electrodes are made by thermally evaporating indium−gold (5:1 volume ratio) metal. The device fabrication details are provided in the Supporting Information.

DOI: 10.1021/acs.chemmater.7b04689
Chem. Mater. 2018, 30, 2544−2549

The charge transfer revealed by UPS impacts the electronic properties found in the TFTs; namely, those made of PbSe-in-SnS_2, PbSe-in-ZnTe, and PbSe-in-$(N_2H_5)_4Ge_2S_6$ nanocomposites exhibit n-type, p-type, and ambipolar carrier transport, respectively. For each of these TFTs, the plots of drain current (I_D) versus drain voltage (V_D) for different representative gate voltages (V_G) are presented in Figure 3. Additional device data and fabrication are discussed in the Supporting Information, Figures S3−S6. In each case, a linear and saturation regime is observed, and the carrier type is reproducibly set by the surface transfer doping process. Although the mobilities are not competitive with the best NC-derived transistors reported in the literature,[13,14,32] the device characteristics demonstrate a clear connection between the nanointerfacial charge transfer revealed by UPS and macroscopically observable electronic behavior. Hence, surface transfer doping can be effectively leveraged to manipulate the electronic transport properties of nanocomposites fabricated so as to control bonding and structure from the atomic through the macroscale.

Charge transfer from an inorganic matrix to NCs can be viewed as remote doping,[33−36] because the transfer of carriers to the active region is spatially separated from the dopant. Indeed, our method bears some similarity to the experiments that report doping of carriers from surface ligands to the semiconductor NC core.[3,8] More generally, recent research efforts points toward a "toolbox" that explores and combines different surface chemistries to design electronic devices with specific properties. These efforts require an investigation of the band alignment and dipoles arising at the interface. For example, Bulović et al.[3] focused on measuring the energy level shifts for various molecular surface species. In a similar study, Chuang et al.[8] reported interface dipoles that cause an abrupt shift in potential across the interface between two layers of identical PbS NCs, one capped with TBAI and another with EDT. The engineering of band alignment at the PbS-TBAI/PbS-EDT interface is crucial for the design of high-performance quantum dot solar cells. Our work on engineering the band alignment at the interface of inorganic matrix/ChaMs to nanocrystals also contributes to the development of the aforementioned toolbox.

As the aim of this study was to elucidate the influence of interfacial charge transfer on carrier type in inorganic nanocomposites, we did not attempt to maximize the mobility or other device performance metrics, which could be accomplished by minimizing charge traps at the nanocomposite and dielectric interfaces, adding excessive ChaMs ligands to act as "molecular solder",[6] or fine-tuning the annealing conditions for the matrix material.[6] Applying these improvements is likely to significantly enhance the device performance and will form part of our future research efforts in this area.

To summarize, in this work we unveiled the electronic reconstruction at the interface in NIM composites and its impact on macroscopically observable electronic behavior. We systematically tuned the electronic reconstruction occurring at the NC−matrix interface to regulate surface charge transfer doping of the embedded PbSe NCs. Analysis of transport in TFTs shows that by choosing appropriate matrix materials, the carrier type can be modulated. This confirms our hypothesis regarding the direct influence that the interface has on transport properties in NIM composites via surface charge transfer doping. Thus, *interactions* between the component materials play a dominant role in determining the overall material properties. Our findings point toward a new and flexible design paradigm for electronic materials.

■ ASSOCIATED CONTENT

Supporting Information

The Supporting Information is available free of charge on the ACS Publications website at DOI: 10.1021/acs.chemmater.7b04689.

Details of experimental setups, measurements, and interpretation (PDF)

■ AUTHOR INFORMATION

Corresponding Author

*(D.J.M.) E-mail: milliron@che.utexas.edu.

ORCID

Angang Dong: 0000-0002-9677-8778
Anna Llordes: 0000-0003-4169-9156
Jeffrey J. Urban: 0000-0002-6520-830X
Delia J. Milliron: 0000-0002-8737-451X

Present Address

⊥(R.S.) Schlumberger-Doll Research, 1 Hampshire Street, Cambridge, Massachusetts 02139, United States.

Notes

The authors declare no competing financial interest.

■ ACKNOWLEDGMENTS

This research was supported by the Welch Foundation (F-1848) and made use of the Molecular Foundry and the Advanced Light Source at Lawrence Berkeley National Laboratory, both user facilities funded by the Office of Science, Office of Basic Energy Sciences, of the U.S. Department of Energy (DOE), under Contract DE-AC02-05CH11231, as well as the Stanford Synchrotron Radiation Lightsource.

■ REFERENCES

(1) Koh, W.; Koposov, A. Y.; Stewart, J. T.; Pal, B. N.; Robel, I.; Pietryga, J. M.; Klimov, V. I. Heavily Doped N-Type PbSe and PbS Nanocrystals Using Ground-State Charge Transfer from Cobaltocene. *Sci. Rep.* **2013**, *3*, 2004.

(2) Ocier, C. R.; Whitham, K.; Hanrath, T.; Robinson, R. D. Chalcogenidometallate Clusters as Surface Ligands for Pbse Nanocrystal Field-Effect Transistors. *J. Phys. Chem. C* **2014**, *118*, 3377−3385.

(3) Brown, P. R.; Kim, D.; Lunt, R. R.; Zhao, N.; Bawendi, M. G.; Grossman, J. C.; Bulović, V. Energy Level Modification in Lead Sulfide Quantum Dot Thin Films through Ligand Exchange. *ACS Nano* **2014**, *8*, 5863−5872.

(4) Ibáñez, M.; Luo, Z.; Genç, A.; Piveteau, L.; Ortega, S.; Cadavid, D.; Dobrozhan, O.; Liu, Y.; Nachtegaal, M.; Zebarjadi, M.; et al. High-Performance Thermoelectric Nanocomposites from Nanocrystal Building Blocks. *Nat. Commun.* **2016**, *7*, 10766.

(5) Milliron, D. J. Quantum Dot Solar Cells: The Surface Plays a Core Role. *Nat. Mater.* **2014**, *13*, 772−773.

(6) Jang, J.; Dolzhnikov, D. S.; Liu, W.; Nam, S.; Shim, M.; Talapin, D. V. Solution-Processed Transistors Using Colloidal Nanocrystals with Composition-Matched Molecular "Solders": Approaching Single Crystal Mobility. *Nano Lett.* **2015**, *15*, 6309−6317.

(7) Ocier, C. R.; Whitham, K.; Hanrath, T.; Robinson, R. D. Chalcogenidometallate Clusters as Surface Ligands for Pbse Nanocrystal Field-Effect Transistors. *J. Phys. Chem. C* **2014**, *118*, 3377−3385.

(8) Chuang, C.-H. M.; Brown, P. R.; Bulović, V.; Bawendi, M. G. Improved Performance and Stability in Quantum Dot Solar Cells

DOI: 10.1021/acs.chemmater.7b04689
Chem. Mater. 2018, 30, 2544−2549

Through Band Alignment Engineering. *Nat. Mater.* **2014**, *13*, 796−801.
(9) Mitzi, D. B. Polymorphic One-Dimensional $(N_2H_4)_2ZnTe$: Soluble Precursors for the Formation of Hexagonal or Cubic Zinc Telluride. *Inorg. Chem.* **2005**, *44*, 7078−7086.
(10) Mitzi, D. B. Synthesis, Structure, and Thermal Properties of Soluble Hydrazinium germanium(IV) and tin(IV) Selenide Salts. *Inorg. Chem.* **2005**, *44*, 3755−3761.
(11) Mitzi, D. B.; Kosbar, L. L.; Murray, C. E.; Copel, M.; Afzali, A. High-Mobility Ultrathin Semiconducting Films Prepared by Spin Coating. *Nature* **2004**, *428*, 299−303.
(12) Chen, W.; Qi, D.; Gao, X.; Wee, A. T. S. Surface Transfer Doping of Semiconductors. *Prog. Surf. Sci.* **2009**, *84*, 279−321.
(13) Lee, J.-S.; Kovalenko, M. V.; Huang, J.; Chung, D. S.; Talapin, D. V. Band-like Transport, High Electron Mobility and High Photoconductivity in All-Inorganic Nanocrystal Arrays. *Nat. Nanotechnol.* **2011**, *6*, 348−352.
(14) Kovalenko, M. V.; Scheele, M.; Talapin, D. V. Colloidal Nanocrystals with Molecular Metal Chalcogenide Surface Ligands. *Science* **2009**, *324*, 1417−1420.
(15) Sharma, R.; Sawvel, A. M.; Barton, B.; Dong, A.; Buonsanti, R.; Llordes, A.; Schaible, E.; Axnanda, S.; Liu, Z.; Urban, J. J.; et al. Nanocrystal Superlattice Embedded within an Inorganic Semiconducting Matrix by in Situ Ligand Exchange: Fabrication and Morphology. *Chem. Mater.* **2015**, *27*, 2755−2758.
(16) Cargnello, M.; Johnston-Peck, A. C.; Diroll, B. T.; Wong, E.; Datta, B.; Damodhar, D.; Doan-Nguyen, V. V. T.; Herzing, A. a.; Kagan, C. R.; Murray, C. B. Substitutional Doping in Nanocrystal Superlattices. *Nature* **2015**, *524*, 450−453.
(17) Owen, J. The Coordination Chemistry of Nanocrystal Surfaces. *Science* **2015**, *347*, 615−616.
(18) Boneschanscher, M. P.; Evers, W. H.; Geuchies, J. J.; Altantzis, T.; Goris, B.; Rabouw, F. T.; van Rossum, S. A. P.; van der Zant, H. S. J.; Siebbeles, L. D. A.; Van Tendeloo, G.; et al. Long-Range Orientation and Atomic Attachment of Nanocrystals in 2D Honeycomb Superlattices. *Science* **2014**, *344*, 1377−1380.
(19) Hassinen, A.; Moreels, I.; De Nolf, K.; Smet, P. F.; Martins, J. C.; Hens, Z. Short-Chain Alcohols Strip X-Type Ligands and Quench the Luminescence of PbSe and CdSe Quantum Dots, Acetonitrile Does Not. *J. Am. Chem. Soc.* **2012**, *134*, 20705−20712.
(20) Sykora, M.; Koposov, A. Y.; Mcguire, J. a.; Schulze, R. K.; Tretiak, O.; Pietryga, J. M.; Klimov, V. I. Effect of Air Exposure on Surface Properties, Electronic Structure, and Carrier Relaxation in PbSe Nanocrystals. *ACS Nano* **2010**, *4*, 2021−2034.
(21) Rosen, E. L.; Buonsanti, R.; Llordes, A.; Sawvel, A. M.; Milliron, D. J.; Helms, B. A. Exceptionally Mild Reactive Stripping of Native Ligands from Nanocrystal Surfaces by Using Meerwein's Salt. *Angew. Chem., Int. Ed.* **2012**, *51*, 684−689.
(22) Liu, Y.; Gibbs, M.; Puthussery, J.; Gaik, S.; Ihly, R.; Hillhouse, H. W.; Law, M. Dependence of Carrier Mobility on Nanocrystal Size and Ligand Length in PbSe Nanocrystal Solids. *Nano Lett.* **2010**, *10*, 1960−1969.
(23) Kang, M. S.; Lee, J.; Norris, D. J.; Frisbie, C. D. High Carrier Densities Achieved at Low Voltages in Ambipolar PbSe Nanocrystal Thin-Film Transistors. *Nano Lett.* **2009**, *9*, 3848−3852.
(24) Mitzi, D. *Solution Processing of Inorganic Materials*; John Wiley & Sons, Inc.: 2009.
(25) Buch, F.; Fahrenbruch, A. L.; Bube, R. H. Photovoltaic Properties of N-CdSe/P-ZnTe Heterojunctions. *Appl. Phys. Lett.* **1976**, *28*, 593−595.
(26) George, J.; Valsala Kumari, C. K.; Joseph, K. S. Absorption Edge of Tin Disulfide Single Crystals. *J. Appl. Phys.* **1983**, *54*, 5347.
(27) Jiang, X.; Schaller, R. D.; Lee, S. B.; Pietryga, J. M.; Klimov, V. I.; Zakhidov, A. A. PbSe Nanocrystal/Conducting Polymer Solar Cells with an Infrared Response to 2 Micron. *J. Mater. Res.* **2007**, *22*, 2204−2210.
(28) Choi, J. J.; Lim, Y. F.; Santiago-Berrios, M.; Oh, M.; Hyun, B. R.; Sun, L.; Bartnik, A. C.; Goedhart, A.; Malliaras, G. G.; Abruña, H. D.; et al. PbSe Nanocrystal Excitonic Solar Cells. *Nano Lett.* **2009**, *9*, 3749−3755.
(29) Flores, F.; Tejedor, C. On the Formation of Semiconductor Interfaces. *J. Phys. C: Solid State Phys.* **1987**, *20*, 145−175.
(30) Flores, F.; Ortega, J.; Vázquez, H. Modelling Energy Level Alignment at Organic Interfaces and Density Functional Theory. *Phys. Chem. Chem. Phys.* **2009**, *11*, 8658.
(31) Wang, R. Y.; Tangirala, R.; Raoux, S.; Jordan-sweet, J. L.; Milliron, D. J. Ionic and Electronic Transport in Ag_2S Nanocrystal−GeS_2 Matrix Composites with Size-Controlled Ag_2S Nanocrystals. *Adv. Mater.* **2012**, *24*, 99−103.
(32) Oh, S. J.; Berry, N. E.; Choi, J.-H.; Gaulding, E. A.; Lin, H.; Paik, T.; Diroll, B. T.; Muramoto, S.; Murray, C. B.; Kagan, C. R. Designing High-Performance PbS and PbSe Nanocrystal Electronic Devices through Stepwise, Post-Synthesis, Colloidal Atomic Layer Deposition. *Nano Lett.* **2014**, *14*, 1559−1566.
(33) Norris, D. J.; Efros, A. L.; Erwin, S. C. Doped Nanocrystals. *Science* **2008**, *319*, 1776−1779.
(34) Shim, M.; Guyot-Sionnest, P. N-Type Colloidal Semiconductor Nanocrystals. *Nature* **2000**, *407*, 981−983.
(35) Oh, S.; Kim, D.; Kagan, C. Remote Doping and Schottky Barrier Formation in Strongly Quantum Confined Single PbSe Nanowire Field-Effect Transistors. *ACS Nano* **2012**, *6*, 4328−4334.
(36) Voznyy, O.; Zhitomirsky, D.; Stadler, P.; Ning, Z.; Hoogland, S.; Sargent, E. H. A Charge-Orbital Balance Picture of Doping in Colloidal Quantum Dot Solids. *ACS Nano* **2012**, *6*, 8448−8455.

DOI: 10.1021/acs.chemmater.7b04689
Chem. Mater. 2018, 30, 2544−2549